

Reference-Based Video Colorization with Spatiotemporal Correspondence

Naofumi Akimoto Akio Hayakawa Andrew Shin Takuya Narihira
Sony Corporation
Tokyo, Japan

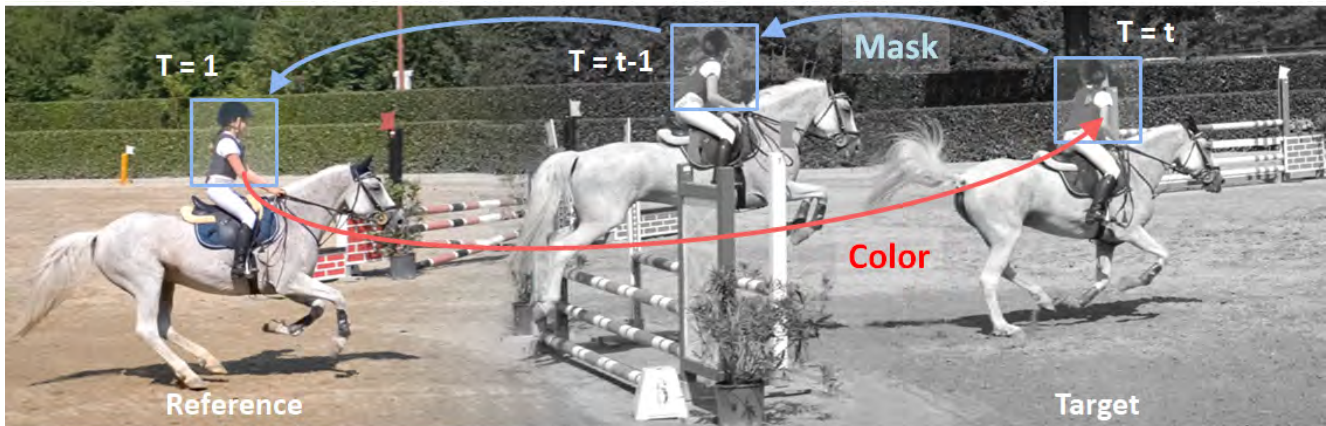


Figure 1: We propose a novel reference-based video colorization framework with spatiotemporal correspondence. We propagate a mask as correspondence in time, and then warp colors with spatial correspondence only from the regions on the reference frame restricted by the temporal correspondence. Our framework realizes faithful and long-term colorization.

Abstract

We propose a novel reference-based video colorization framework with spatiotemporal correspondence. Reference-based methods colorize grayscale frames referencing a user input color frame. Existing methods suffer from the color leakage between objects and the emergence of average colors, derived from non-local semantic correspondence in space. To address this issue, we warp colors only from the regions on the reference frame restricted by correspondence in time. We propagate masks as temporal correspondences, using two complementary tracking approaches: off-the-shelf instance tracking for high performance segmentation, and newly proposed dense tracking to track various types of objects. By restricting temporally-related regions for referencing colors, our approach propagates faithful colors throughout the video. Experiments demonstrate that our method outperforms state-of-the-art methods quantitatively and qualitatively.

1. Introduction

Colorizing black-and-white videos has increasingly gained attention, since it can revitalize a massive amount of outdated contents into modern standards. Previously, pro-

duction of high-quality contents has required manual colorization, resulting in prohibitively high costs in terms of time and labor. Researchers have thus endeavored to come up with a scheme to automate the colorization process, in fully automatic [14] or semi-automatic ways [7, 31]. Yet, video colorization remains a highly challenging task. On top of the challenging aspects of image colorization, such as its ill-posed nature with a large number of potentially correct results, video colorization imposes additional dimensions of challenge, namely maintaining temporal coherence, computational cost, and user controllability.

Recent attention-based approaches [7, 31] proposed to compute correspondence between the target frame and reference frame using semantic features, and colorize the target frame by attending to the color from reference frame. This approach can alleviate the issue of accumulating mispredictions over the frames, which is prevalent in propagation-based approaches [11, 17]. However, as shown in Fig. 5, its non-local spatial correspondence frequently results in color leakage between instances, or the objects colorized with average colors from multiple objects.

To address this issue, we instead propose a reference-based video colorization with spatiotemporal correspondence. The key assumption of our work is that, by assigning color to objects that exist in both reference and target frames

with finer correspondence, we can enhance video colorization, as illustrated in Fig. 1. However, if attention-based model is augmented in an incremental manner by warping the color from both reference frame and previous frame, it inevitably results in placing higher priority for previous frame, since it tends to resemble the target frame more. As a result, it is likely to be degraded to propagation-based model. We thus need another approach to account for the *continuity* of regions over temporal axis, while avoiding the errors from accumulated color propagation.

Our key ideas to tackle this technical issue are as following: 1) propagate masks to represent the correspondence over time axis instead of color, and 2) color is determined within the region restricted by the mask in the reference frame. Fig. 2 illustrates the differences between our model and others. Our framework consists of three stages, namely tracking, warping, and refinement. Tracking is performed in order to obtain the temporal correspondence between reference frame and target frame. We can specify which color to warp more accurately, by specifying the region in reference frame that is temporally correlated to pixels to colorize on target frame. For warping color, we obtain semantic features by feeding reference and target frames to the network, and compute the spatial correspondence based on their similarity. Furthermore, by warping the color solely from the region specified by tracking, we can warp the color based on spatiotemporal correspondence. In contrast to propagation-based models in which the succeeding frames may be colored with incorrect color due to accumulation of prediction error over the frames, our model can perform colorization with vivid color specified by reference frame via propagating masks rather than colors. Finally, refinement stage employs encoder-decoder network to recover the mistakes from warping colors and enhance the temporal coherence throughout neighboring frames.

Moreover, we propose to incorporate two types of tracking as a way to obtain correspondence over temporal axis, which restricts the region to warp color from. We first employ 1) instance tracking in order to prevent incorrectly blending the colors from distinct objects. To the best of our knowledge, our model is the first video colorization work that is instance-aware. By using instance tracking, we can accurately differentiate between instances. However, instance tracking alone cannot track objects of undefined classes, or track at granularity smaller than the instance. In order to resolve such issues, 2) we propose a mechanism to track at pixel-level. Inspired by dense tracking [27], we exploit correspondence learned from colorization for tracking without having to further train the model. By specifying temporally correlated regions for each pixel, we can avoid the problem of blurry colors resulting from warping color from the entire frame.

Through the approaches above, our proposed model is

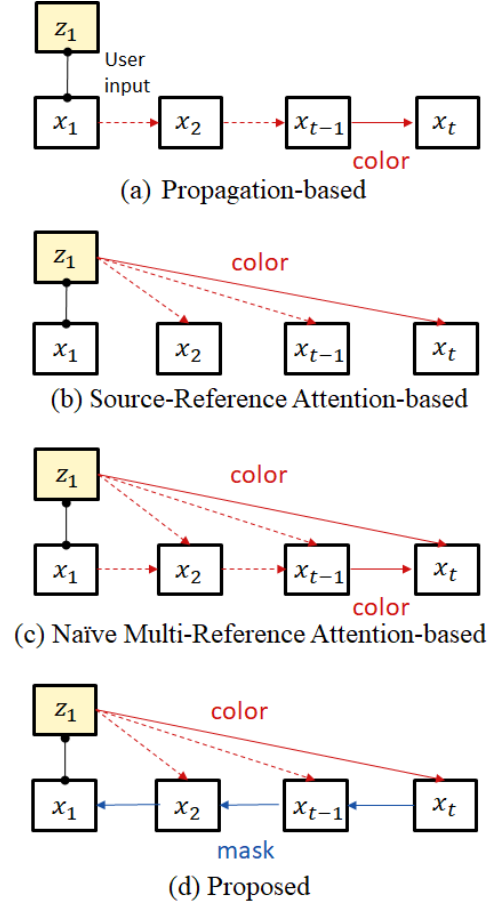


Figure 2: Comparison among four types of approaches when processing an input video x with reference frame z . The figures illustrate a user colorizing x_1 with a reference frame z_1 . (a) and (c) suffer accumulation error, because they colorize x_t with colored x_{t-1} . See Fig. 7 for a visualization of (c). (d) warp colors considering temporal correspondence between x_t and z_1 , unlike (b).

capable of high-quality colorization for videos of long duration with complex scenes, frequently involving change in background or rapid movement of objects. Its faithful reflection of reference also leads to reduced amount of manual work and enhanced user controllability. Experiment results clearly demonstrate that our model outperforms state-of-the-art-models both quantitatively and qualitatively. In particular, our spatiotemporal correspondence turns out to be effective when dealing with complex scenes that attention-based approach finds difficult.

Our contributions can be summarized as following:

- We propose a novel reference-based video colorization framework with spatiotemporal correspondence. We propagate a mask as correspondence in time, and warp colors with spatial correspondence from the regions restricted by the temporal correspondence.
- We propose a novel dense tracking specialized for video colorization. With no additional training, it

faithfully reflects the color from user reference.

- Our proposed method outperforms state-of-the-art methods and improves user-controllability, while alleviating color leakage or color being averaged out.

2. Related Work

Image Colorization. Early image colorization was mostly performed with user-guided signatures and sample references [3, 6, 19, 24]. These methods propagate local color guidance to similar regions using low-level features. They frequently relied on deep-learning in fully automatic manner to learn the semantic-color relationships from a large dataset [8, 9, 32], or to propagate the user-guided scribbles in the spatial direction based on the semantic feature [33], or warp the color to a corresponding position based on exemplar color sample [5]. Recently, as a new perspective, an instance-aware approach has been proposed for image colorization [26]. Learning instance-color relationships improves the performance of fully automatic image colorization. We extend the instance-aware approach for video colorization.

Video Colorization. Video colorization is far more difficult than image colorization and is still an open challenge. An intuitive approach is to perform post processing [1, 12] to impose temporal coherence to flickers of per-frame colorization, but the colors are likely to be washed out. The propagation of color scribbles [15, 30] or a colored first frame [11, 17, 27] across frames using estimated flow may suffers from accumulation of errors, and consequently, the number of frames that can be propagated is limited.

Recently, source-reference attention-based methods [7, 31] has been proposed. Accumulation of errors is reduced by using a reference image for coloring each frame instead of using the last colored frame. However, there exists no direct handling of temporal information for correspondence. These methods warp colors solely based on the relationship to a reference frame, and then consider the relationship between target frames for temporal coherence. Due to non-local attention, colors are frequently mixed even between objects that should be distinguished. Conversely, our method warps a color from a part of a reference frame by limited correspondence based on temporal information of the target frame. This makes it possible to determine a color only from a similar region in the nearest neighbor in space and time, resulting in a colorization without a color leakage between instances and a faithful colorization for the reference image.

Dense Tracking. Dense tracking is a task that re-localizes objects in the preceding and succeeding frames with pixel-level segmentation masks. Recent self-supervised learning methods trained with video colorization [10, 13, 16, 27] or cycle consistency [28, 29] propagate a given segmentation mask to subsequent frames based on

the correspondences. In video colorization task, however, we cannot use methods that require pre-processed object’s masks provided by user as input [2, 20, 21], or methods that use color information [10, 18]. To improve colorization at pixel-level, we need masks for each pixel of the target frame separately, rather than tracking several representative object masks. Our newly proposed dense tracking method is designed to be applicable to such requirements of colorization task, inspired by the method [27], as we describe in Sec. 3.4.

3. Method

3.1. Overview

We propose a reference-based video colorization framework which consists of three stages; a tracking stage, a spatially restricted color warping stage, and a color refinement stage. Fig. 3 shows the overview of our framework. Inputs for the whole system are grey-scale frames $x^l = \{x_t^l\}_{t=1}^{t=N}$ where $x_t^l \in \mathbb{R}^{H \times W \times 1}$, and some colored reference frames picked from the video are $y^{ab} = \{y_r^{ab}\}_{r=1}^{N_{\text{ref}}}$ where $y_r^{ab} \in \mathbb{R}^{H \times W \times 2}$, and the outputs are the chrominance ab for each frame $\hat{x}^{ab} = \{\hat{x}_t^{ab}\}_{t=1}^{t=N}$ where $\hat{x}_t^{ab} \in \mathbb{R}^{H \times W \times 1}$.

To obtain a mask for restricting regions to calculate correspondence, we execute instance tracking (Sec. 3.3) and dense tracking (Sec. 3.4). We warp colors based on an affinity matrix $A \in [0, 1]^{HW \times HW}$ between semantic features of a target frame x_t^l and a reference frame y_r^l . To colorize the target frame with colors faithful for the reference frame, we calculate a semantic correspondence only among regions which have temporal relations, instead of non-local semantic correspondence (Sec. 3.2). To do so, we use the tracking masks for each reference frame $M = \{M_r\}_{r=1}^{N_{\text{ref}}}$ where $M_r \in \{0, 1\}^{HW \times HW}$, which captures temporal information among the target frames. Furthermore, we extend this mechanism to handle multiple reference images. Namely, we calculate warped colors $W_t^{ab} \in \mathbb{R}^{H \times W \times 2}$ for target frame x_t by warping function F as follows:

$$W_t^{ab} = F(x_t^l, y_1^{ab}, M_1, \dots, y_{N_{\text{ref}}}^{ab}, M_{N_{\text{ref}}}) \quad (1)$$

Note that M_r here represents tracking result of y_r propagated from t -th frame x_t . For all frames $\{x_t\}_{t=1}^N$, we calculate different masks from target frames to each reference frame in the same way. For simplicity, we hereinafter omit x_t and y_r and refer to M_r as a mask between a target frame x_t and a reference frame y_r .

In color refinement stage, we use fully-convolutional u-net proposed in Zhang *et al.* [32]. This network refines the warp result to have temporal coherence with the consecutive frame and improves spatial consistency. The inputs for the refinement network are the colored last frame \hat{x}_{t-1} , the warp result of the frame to be colorized W_t^{ab} , and the warp confidence map $S_t \in [0, 1]^{H \times W}$ that is max values of the affinity matrix for the reference dimension. This refinement

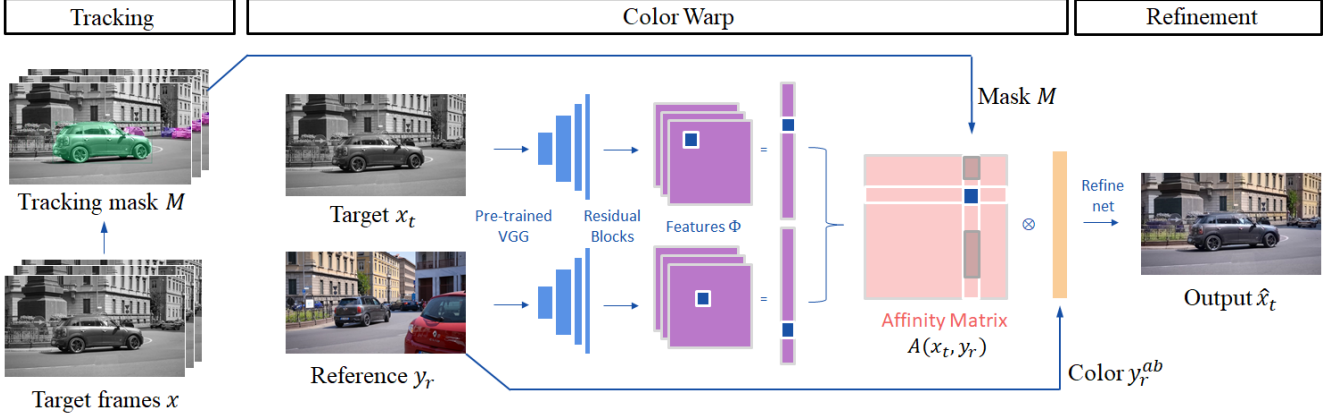


Figure 3: Pipeline overview. Our framework consists of three stages: tracking stage for obtaining a mask as a temporal correspondence between target frames (Sec. 3.3 and Sec. 3.4), color warping stage for coloring a target frame with the tracking mask (Sec. 3.2, and refinement stage for temporal coherence.

function G can be expressed as:

$$\hat{x}_t^{ab} = G(x_{t-1}^l, x_t^l, \hat{x}_{t-1}^{ab}, W_t^{ab}, S_t) \quad (2)$$

3.2. Spatially restricted Correspondence

In this section, we present the calculation of semantic correspondence at first, and the calculation of the correspondence restricted by the tracking mask with temporal information, and extend the mechanism to handle multiple references.

To obtain the semantic correspondence between target frame x_t and reference frame y_r , we transfer the target frame and the reference frame to VGG network [25] features, and concatenate features from multiple layers. Feeding them into further residual blocks, we extract features $\Phi(x_t), \Phi(y_r) \in \mathbb{R}^{HW \times L}$, respectively. Note that we use only luminance l for both x_t and y_r to calculate $\Phi(x_t), \Phi(y_r)$. Using $\Phi(x_t)$ and $\Phi(y_r)$, we calculate the affinity matrix A of the target frame and the reference frame from correlation matrix $C \in \mathbb{R}^{HW \times HW}$ as follows:

$$A(x_t, y_r) = \text{softmax}_j(C(x_t, y_r)) \quad (3)$$

$$C_{i,j}(x_t, y_r) = \frac{(\Phi_i(x_t) - \mu_{\Phi_{x_t}})^T (\Phi_j(y_r) - \mu_{\Phi_{y_r}})}{\|\Phi_i(x_t) - \mu_{\Phi_{x_t}}\|_2 \|\Phi_j(y_r) - \mu_{\Phi_{y_r}}\|_2} \quad (4)$$

where, $\mu_{\Phi_{x_t}}$ and $\mu_{\Phi_{y_r}}$ represent mean feature vectors. Based on this affinity matrix, we calculate warped colors from reference frame to target frame by the product of the affinity matrix and the ab vector of the reference frame. Thus, in the setting with a single reference frame, equation 1 can be represented as:

$$W_t^{ab}(i) = \sum_j A_{i,j}(x_t, y_r) y_r^{ab}(j) \quad (5)$$

where $W_t^{ab}(i) \in \mathbb{R}^2$ is a chrominance ab of the i -th position at t -th frame and $y_r^{ab}(j) \in \mathbb{R}^2$ is that of the j -th position at a reference frame y_r^{ab} .

This algorithm relates the target frame and the reference frame to each other in non-local regions, without considering their temporal relation. However, our objective is to determine the colors only from the regions that are estimated to be relevant based on the time information. To do so, we use a tracking mask based on the time series relationship for this affinity matrix to limit the candidates. Specifically, we replace A in equation 6 with a restricted affinity matrix $\tilde{A} \in [0, 1]^{HW \times HW}$ that is:

$$W_t^{ab}(i) = \sum_j \frac{\tilde{A}_{i,j}(x_t, y_r, M_r)}{\sum_{i'} \tilde{A}_{i',j}(x_t, y_r, M_r)} y_r^{ab}(j) \quad (6)$$

$$\tilde{A}_{i,j}(x_t, y_r, M_r) = \begin{cases} A_{i,j}(x_t, y_r) & \text{if } M_{r,i,j} = 1 \\ 0, & \text{otherwise} \end{cases} \quad (7)$$

This suggests that we require the masks M_r on the reference frame to correspond to each target pixel. As a way to prepare tracking masks containing temporal relations, we propose two approaches: using masks from instance tracking (Sec. 3.3) and using masks from a dense tracking (Sec. 3.4). We describe masks obtained by these two approaches as M^I and M^D in the following sections.

Considering a practical application, the method using a single reference as in [31] is likely insufficient because there are many colors that cannot be specified when working with long videos in which many new colors and objects appear. To address this issue, we extend the model to deal with multiple references. In this case, the equation 6 can be extended by multiple references y and masks M as follows:

$$W_t^{ab}(i) = \sum_{r,j} \frac{\tilde{A}_{r,i,j}^m(x_t, y, M)}{\sum_{i'} \tilde{A}_{r,i',j}^m(x_t, y, M)} y_r^{ab}(j) \quad (8)$$

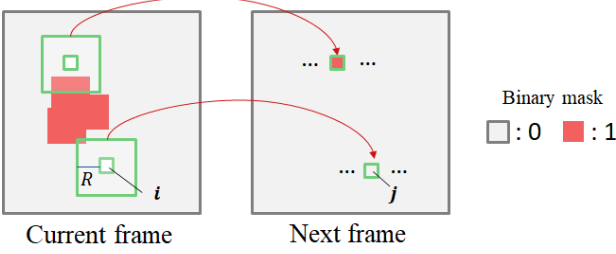


Figure 4: Mask propagation by dense tracking. Our method propagates a mask to the next frame when the similarity between a pixel on the next frame and the neighborhood on the current frame exceeds a threshold.

where $\tilde{A}^m, A^m \in [0, 1]^{N_{\text{ref}} \times HW \times HW}$ is a restricted and non-restricted stacked affinity matrix and $C^m \in \mathbb{R}^{N_{\text{ref}} \times HW \times HW}$ is a stacked correlation matrix such as:

$$\tilde{A}_{r,i,j}^m(x_t, y, M) = \begin{cases} A_{r,i,j}^m(x_t, y) & \text{if } M_{r,i,j} = 1 \\ 0, & \text{otherwise} \end{cases} \quad (9)$$

$$A^m(x_t, y) = \text{softmax}_{r,j}(C^m(x_t, y)) \quad (10)$$

$$C^m(x_t, y) = \text{stack}(C(x_t, y_1), \dots, C(x_t, y_{N_{\text{ref}}})) \quad (11)$$

3.3. Instance Tracking

To solve the problem of warping color between instances, we use off-the-shelf pre-trained instance segmentation [4] to calculate an instance mask for each frame, and then use IoU (Intersection over Union) of each mask between adjacent frames to identify the same instance. First, using this tracking function T , we obtain instance tracking masks $\{I'_t(k)\}_{t=1}^N \in [0, 1]^{HW}$ as vectors for each object $k \in \{1, 2, \dots, N_{\text{obj}}\}$:

$$I'_1(k), \dots, I'_N(k) = T(I_1(k), \dots, I_N(k)) \quad (12)$$

where $\{I_t(k)\} \in [0, 1]^{HW}$ is an instance mask of object k in t -th frame. Let $\phi_i(x_t) \in \{1, 2, \dots, N_{\text{obj}}\}$ be a function to get a label id at i -th position of target frame x_t . Finally, we calculate an instance tracking mask $M^I \in [0, 1]^{HW \times HW}$ for a reference frame y_r to limit affinity between x_t and y_r as follows:

$$M_{r,i,j}^I = \begin{cases} 1 & \text{if } I'_{r,j}(\phi_i(x_t)) \geq \text{threshold} \\ 0 & \text{otherwise} \end{cases} \quad (13)$$

3.4. Dense Tracking

Because instance tracking can only handle instances of classes that are already defined, it is not possible to capture temporal relationships of regions of non-defined classes, or areas other than the instance. To compensate for this

limitation and make the color of the reference frame faithful across the image, we introduce dense tracking. Previous studies of self-supervised dense tracking have shown that trackers can be learned by training reference-based colorization [27]. Since we already have a correspondence mechanism for video colorization, we can use dense tracking without additional training.

The difference in setting from [27] is that it is necessary to individually track each pixel of the frame to be colored, instead of tracking a set of pixels. In [27], a set of pixels is specified as an object mask for the first frame to track. Conversely, in our task, the individual pixels of the target to be colored are the target of tracking. We thus need to propose a new dense tracking algorithm since the mask would disappear immediately when we directly use the existing method for our task.

Fig. 4 visualizes how we propagate masks using dense tracking. To calculate the mask $M_r^D \in \mathbb{R}^{HW \times HW}$, which represents candidate positions at a reference frame r to warp to the i -th position of x_t , we repeat propagating a mask from a target x_t to a reference y_r . Let $t' \in \{t, t+1, \dots, t_r\}$ be a set of frame indices from x_t to y_r , where t_r represents a frame index of y_r , and $D^{t'}(i_0) \in \{0, 1\}^{HW}$ be propagated candidate positions at t' -th frame from the i_0 -th position of x_t . We define the initial mask at $t' = t$ as it has value 1 only at $i = i_0$ position otherwise 0:

$$D_i^{t'}(i_0) = \begin{cases} 1 & \text{if } i = i_0 \\ 0 & \text{otherwise} \end{cases} \quad (14)$$

Assuming that the moving destination of the pixel exists in the nearest neighbors, we propagate candidate positions from the i_0 -th position of x_t to a reference frame y_r by following equations:

$$D_j^{t'}(i_0) = \text{binarize} \left(\frac{\sum_i A_{i,j}^D(x_{t'-1}, x_{t'})}{\sum_{j'} A_{i,j'}^D(x_{t'-1}, x_{t'})} D_i^{t'-1}(i_0) \right) \quad (15)$$

$$A_{i,j}^D(x_{t'-1}, x_{t'}) = \begin{cases} A_{i,j}(x_{t'-1}, x_{t'}) & \text{if } j \in \mathcal{N}_i^R \\ 0 & \text{otherwise} \end{cases} \quad (16)$$

where $A^D \in [0, 1]^{HW \times HW}$ is a spatially restricted affinity, and \mathcal{N}_i^R is a set of neighboring pixels residing within the window whose size is $2R \times 2R$ centered at i -th position. Here, R is a hyperparameter to limit neighbors. Propagating masks from t -th frame to t_r -th frame, we calculate a dense tracking mask $M_r^D \in \{0, 1\}^{HW \times HW}$ for a reference frame y_r as follows:

$$M_{r,i,j}^D = \begin{cases} 1 & \text{if } D_j^{t_r}(i) = 1 \\ 0 & \text{otherwise} \end{cases} \quad (17)$$

As described in equation 15, in order to generate many candidates for tracking destinations, we convert pixels,

Method	Single Reference			Multiple References					
	10th frame			1st & Nth frames			10th & N-10th frames		
	Full	Inner	Outer	Full	Inner	Outer	Full	Inner	Outer
DeepRemaster [7]	25.53	24.44	25.70	25.38	24.18	25.60	25.53	24.40	25.73
Zhang <i>et al.</i> [31]	28.61	27.71	28.72	-	-	-	-	-	-
Zhang <i>et al.</i> [31]* (mean)	-	-	-	28.17	27.17	28.39	28.24	27.30	28.44
Zhang <i>et al.</i> [31]* (linear)	-	-	-	28.35	27.39	28.53	28.54	27.68	28.69
Ours w/o tracking	28.61	27.71	28.72	28.37	27.50	28.54	28.58	27.76	28.73
Ours (inst.)	28.59	27.75	28.70	28.36	27.55	28.52	28.58	27.82	28.72
Ours (dense)	28.74	29.12	27.79	29.27	27.59	28.94	29.02	27.85	29.19
Ours (inst.+dense)	29.13	27.94	29.27	28.74	27.69	28.93	29.03	27.97	29.19

Table 1: PSNR. Higher is better. The first block of three columns shows the results with single reference frame. The remaining two blocks show the results with multi-reference setting. Full, Inner, and Outer refer to the region with respect to instance masks used for evaluation.

whose similarity score exceeds a threshold value, to binary masks as candidates for movement. By creating a one-to-many relationship between the starting point and the destinations of tracking, it encourages the generation of multiple mask candidates, even when starting at only one point in the target. Furthermore, by setting binary masks with threshold, it is possible to prevent the repeated multiplication of the probability from reaching zero, which frequently happens without performing threshold processing.

By repeating the above update from target to reference, for each pixel on the target frame, a mask representing the destination on reference is obtained. As a result, it is possible to restrict regions as a candidate for soft warp of a color.

4. Experiments

4.1. Experimental Setting

Datasets. We mainly report our results on DAVIS-2017 [23]. We refer the readers to Appendix for results on other datasets, as they generally exhibit similar trends. We test video colorization on 90 videos from the training and validation splits. We resize videos to 384×216 , and set window size $R = 9$ and threshold = 0.2 in binarize function. Note that none of the data from DAVIS-2017 are used for training. In DAVIS-2017, ground truth instance segmentations are annotated at pixel level in each frame.

Evaluation Metrics. As with the existing quantitative evaluation protocol for colorization methods, we report the peak signal-to-noise ratio (PSNR) to compare with other methods. It is possible to evaluate whether the color can be propagated faithfully to the reference color since, by providing ground truth colors as a reference frame, it is expected that the ground truth color is propagated to the following frames. Note that video with frequent dynamic changes cannot fully reproduce the ground truth frame because not all colors can be specified in a limited number of reference frames.

Network Training. Since our network relies on [31] as

the backbone, we evaluate it using its distributed parameters to make fair comparisons. The feature extraction network for calculating the correspondence and the refinement network are trained end-to-end using multiple effective losses [31]. As described in Sec 3.1, no additional training is required to perform our dense tracking.

4.2. Comparisons with the state-of-the-art

Quantitative Comparisons. We report the results for PSNR on DAVIS in Table 1. We report experiments with three types of reference frames: 1) single reference of 10th frame from the beginning, 2) multiple references given at the beginning (1st) and the end (N -th) of a sequence, and 3) multiple references at the 10th frame from the beginning and 10th from the end (N -10th). Note that the position of reference frame can be arbitrary, as shown in Appendix. As well as PSNR for the entire image, we also report the evaluations inside and outside the ground truth instance masks on DAVIS. Note that while [7] consists of two networks, a restoration network and a colorization network, we use only the colorization network. Since Zhang *et al.* [31] proposes a workflow for a single reference, in order to compare the multiple reference results with Zhang *et al.* [31], we create the outputs at each reference, and assign them weights either by mean or linearly as the distance between the target and the reference frame. We refer to them as Zhang *et al.* [31]* (mean) and Zhang *et al.* [31]* (linear), respectively.

We report four variations of our method. Ours (w/o tracking) is an extension of Zhang *et al.* [31] to a mechanism for multiple references. When only instance tracking is used (Ours (inst.)), an improvement in the inner of the instance mask is observed. Note that there is a change in the score outside the mask, because the region detected by the instance detector is different from the instance region of the ground truth. Ours (dense) uses dense tracking to improve scores across images. Ours (inst. + dense), which further improved on instance tracking, achieves the highest performance in most cases. These results demonstrate that



Figure 5: Qualitative comparisons with state-of-the-arts with single reference. When there are two car on the reference frame, the body of the car on (b) Zhang *et al.* [31] contains red. On the other hand, (c) ours is not affected by the red car as we identify the car instances, and the color is clearer than (a) DeepRemaster[7].

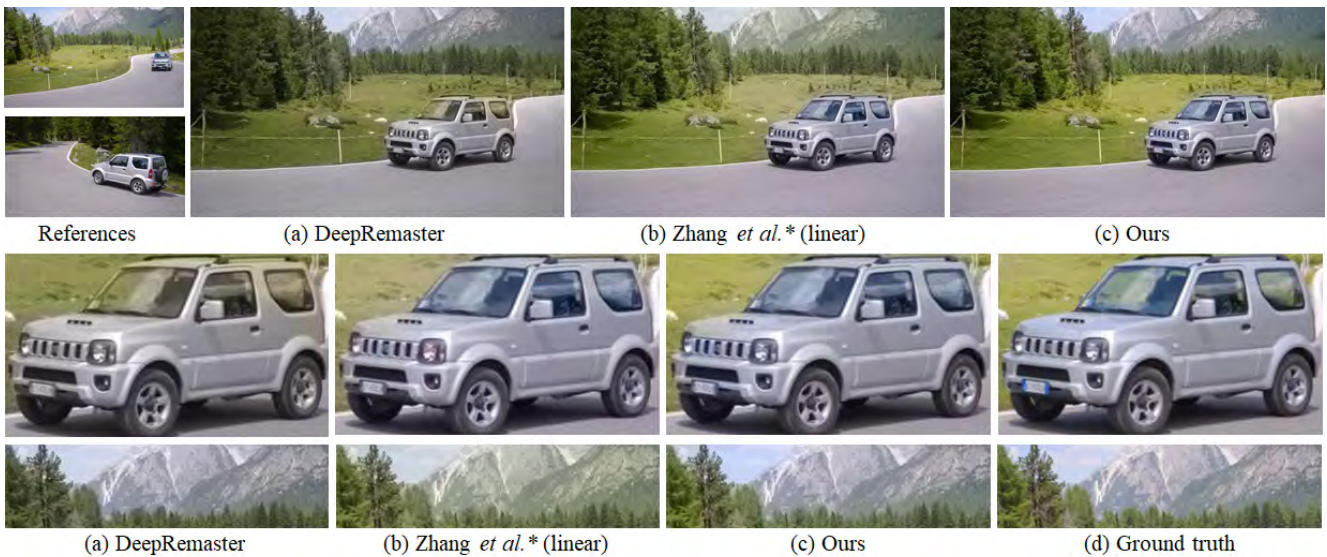


Figure 6: Qualitative comparisons with state-of-the-arts with multiple reference. (a) DeepRemaster[7]’s car is green and the sky and the trees are faded. On (b) Zhang *et al.* [31]* (linear), the car headlight seems red, and the sky and the mountains are green.



Figure 7: Comparison of color propagation and mask propagation. (b) shows the result of Fig. 2(c), and color propagation errors accumulate visibly. Conversely, plausible color can be warped from the reference frame even with an error in the mask propagation (c).

using temporal correspondence and restricting the region to reflect the reference frame improve performance.

Qualitative Comparisons. Fig. 5 and Fig. 6 show comparisons of the results of the proposed method and the state-of-the-art methods. Fig. 5 shows the results when there



Figure 8: A scene where instance tracking is effective.

are the same semantic objects (car) in a reference frame. Zhang *et al.* [31] warps colors from the two cars, and as a result, the car in the target frame incorrectly contains red. The stone tower on the left-hand side of the image also incorrectly contains red. In contrast, our method prevents



Figure 9: Comparison of dense tracking with other methods. (a) Zhang *et al.* [31] using non-local attention struggles with long time or changing objects. (b) Instance detection is not successful in this case, and the result also affects colorization. On the other hand, by tracking on a vehicle-by-vehicle basis, (c) ours (dense) propagates correct colors.

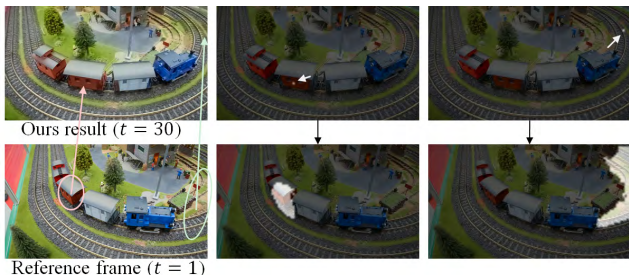


Figure 10: Visualization of dense tracking. We use dense tracking to obtain masks on the reference frame corresponding to each pixel on the target frame. We determine a color of the target pixel by further weighting from masked regions on the reference image.

color transfer from the red car by considering the temporal relationship between frames. In addition, the color is clearer than that of DeepRemaster [7]. As shown in Fig. 6, our method achieves more accurate colorization than other methods even when there are multiple reference images. Our proposed framework with spatiotemporal correspondence improves colorization performance at a finer level than instances, such as the color of the pixel of the sky and mountains.

4.3. Analysis

Spatiotemporal Correspondence. Our approach expresses temporal correspondence as mask propagation. Another approach (Fig. 2(c)) that warps colors from both the reference frame and previous frame tends mostly to use the color of the previous frame because the previous frame is more similar to current target frame than the reference frame. In this method, therefore, it is difficult to colorize a long video due to accumulation of errors, as shown in Fig. 7. On the other hand, our method results in high fidelity and can colorize a long video, by warping the color of the reference frame, while considering the relation between the target frames.

Instance Tracking. Fig. 8 shows the effect of instance tracking. Our model takes advantage of the highly accurate segmentation of off-the-shelf instance detection. Our model can also prevent color leakage between instances even in

long videos. Table 1 shows that the performance can be improved within the ground truth instance mask.

Dense Tracking. Fig. 9 compares dense tracking with other models. Dense tracking tracks every pixel on the target frame. Fig. 10 visualizes dense tracking. As shown in the figures, tracking can be performed regardless of the class or size of the object. The color is determined by calculating the similarity only in the masked region propagated from the target frame to the reference frame. Therefore, while the tracking accuracy is not as high as with instance tracking, the influence of the error can be reduced at the time of warping the color.

Limitations. In our method, thresholds for window to limit neighbors are determined manually for dense tracking. If window size is too large, they can span different instances. On the other hand, if the window size is too small, it is difficult to track an object having a large amount of movement. Therefore, it is necessary to determine a threshold adaptively according to the content of the video. For our future work, we are interested in automating the setting of manual thresholds such as window size.

5. Conclusions

We proposed a novel framework for reference-based video colorization. Our method uses temporal correspondence between target frames to reflect the reference color more faithfully. We also proposed a dense tracking method in addition to the introduction of instance tracking as a method to compute temporal correspondence. Experimental results demonstrate that our model outperforms state-of-the-art models both qualitatively and quantitatively. While it is still challenging to track across different scenes with different camera shots, it may be handled efficiently by detecting scene switches, which remains as our future work.

Acknowledgement

We thank Masato Ishii for helpful discussions and comments. We also thank Sony Pictures Entertainment Technology Development Group for providing data and feedback.

References

- [1] Nicolas Bonneel, James Tompkin, Kalyan Sunkavalli, Deqing Sun, Sylvain Paris, and Hanspeter Pfister. Blind video temporal consistency. *ACM Trans. Graph.*, 34(6), 2015. 3
- [2] Sergi Caelles, Kevis-Kokitsi Maninis, Jordi Pont-Tuset, Laura Leal-Taixé, Daniel Cremers, and Luc Van Gool. One-shot video object segmentation. In *Proceedings of the IEEE conference on computer vision and pattern recognition*, pages 221–230, 2017. 3
- [3] Anat Levin Dani, Dani Lischinski, and Yair Weiss. Colorization using optimization. *ACM Transactions on Graphics*, 23:689–694, 2004. 3
- [4] Kaiming He, Georgia Gkioxari, Piotr Dollar, and Ross Girshick. Mask r-cnn. In *Proceedings of the IEEE International Conference on Computer Vision (ICCV)*, Oct 2017. 5, 11
- [5] Mingming He, Dongdong Chen, Jing Liao, Pedro V Sander, and Lu Yuan. Deep exemplar-based colorization. *ACM Transactions on Graphics (TOG)*, 37(4):47, 2018. 3
- [6] Yi-Chin Huang, Yi-Shin Tung, Jun-Cheng Chen, Sung-Wen Wang, and Ja-Ling Wu. An adaptive edge detection based colorization algorithm and its applications. In *Proceedings of the 13th annual ACM international conference on Multimedia*, pages 351–354, 2005. 3
- [7] Satoshi Iizuka and Edgar Simo-Serra. DeepRemaster: Temporal Source-Reference Attention Networks for Comprehensive Video Enhancement. *ACM Transactions on Graphics (Proc. of SIGGRAPH Asia 2019)*, 38(6), 2019. 1, 3, 6, 7, 8, 12, 13
- [8] Satoshi Iizuka, Edgar Simo-Serra, and Hiroshi Ishikawa. Let there be Color!: Joint End-to-end Learning of Global and Local Image Priors for Automatic Image Colorization with Simultaneous Classification. *ACM Transactions on Graphics (Proc. of SIGGRAPH 2016)*, 35(4), 2016. 3
- [9] Phillip Isola, Jun-Yan Zhu, Tinghui Zhou, and Alexei A Efros. Image-to-image translation with conditional adversarial networks. *CVPR*, 2017. 3
- [10] Allan Jabri, Andrew Owens, and Alexei Efros. Space-time correspondence as a contrastive random walk. *Advances in Neural Information Processing Systems*, 33, 2020. 3
- [11] Varun Jampani, Raghudeep Gadde, and Peter V. Gehler. Video propagation networks. In *IEEE Conf. on Computer Vision and Pattern Recognition (CVPR)*, 2017. 1, 3
- [12] Wei-Sheng Lai, Jia-Bin Huang, Oliver Wang, Eli Shechtman, Ersin Yumer, and Ming-Hsuan Yang. Learning blind video temporal consistency. In *European Conference on Computer Vision*, 2018. 3
- [13] Zihang Lai, Erika Lu, and Weidi Xie. Mast: A memory-augmented self-supervised tracker. In *Proceedings of the IEEE/CVF Conference on Computer Vision and Pattern Recognition*, pages 6479–6488, 2020. 3
- [14] Chenyang Lei and Qifeng Chen. Fully automatic video colorization with self-regularization and diversity. In *The IEEE Conference on Computer Vision and Pattern Recognition (CVPR)*, June 2019. 1
- [15] Anat Levin, Dani Lischinski, and Yair Weiss. Colorization using optimization. In *ACM SIGGRAPH 2004 Papers*, pages 689–694. 2004. 3
- [16] Xueting Li, Sifei Liu, Shalini De Mello, Xiaolong Wang, Jan Kautz, and Ming-Hsuan Yang. Joint-task self-supervised learning for temporal correspondence. In *Advances in Neural Information Processing Systems*, pages 318–328, 2019. 3
- [17] Sifei Liu, Guangyu Zhong, Shalini De Mello, Jinwei Gu, Varun Jampani, Ming-Hsuan Yang, and Jan Kautz. Switchable temporal propagation network. In *Proceedings of the European Conference on Computer Vision (ECCV)*, pages 87–102, 2018. 1, 3
- [18] Xiankai Lu, Wenguan Wang, Jianbing Shen, Yu-Wing Tai, David J Crandall, and Steven CH Hoi. Learning video object segmentation from unlabeled videos. In *Proceedings of the IEEE/CVF Conference on Computer Vision and Pattern Recognition*, pages 8960–8970, 2020. 3
- [19] Qing Luan, Fang Wen, Daniel Cohen-Or, Lin Liang, Ying-Qing Xu, and Heung-Yeung Shum. Natural Image Colorization. In Jan Kautz and Sumanta Pattanaik, editors, *Rendering Techniques*. The Eurographics Association, 2007. 3
- [20] Jonathon Luiten, Paul Voigtlaender, and Bastian Leibe. Premvos: Proposal-generation, refinement and merging for video object segmentation. In *Asian Conference on Computer Vision*, 2018. 3
- [21] K-K Maninis, Sergi Caelles, Yuhua Chen, Jordi Pont-Tuset, Laura Leal-Taixé, Daniel Cremers, and Luc Van Gool. Video object segmentation without temporal information. *IEEE transactions on pattern analysis and machine intelligence*, 41(6):1515–1530, 2018. 3
- [22] Moritz Menze and Andreas Geiger. Object scene flow for autonomous vehicles. In *Conference on Computer Vision and Pattern Recognition (CVPR)*, 2015. 11
- [23] Jordi Pont-Tuset, Federico Perazzi, Sergi Caelles, Pablo Arbeláez, Alexander Sorkine-Hornung, and Luc Van Gool. The 2017 davis challenge on video object segmentation. *arXiv:1704.00675*, 2017. 6, 11
- [24] Yingge Qu, Tien-Tsin Wong, and Pheng-Ann Heng. Manga colorization. *ACM Transactions on Graphics (SIGGRAPH 2006 issue)*, 25(3):1214–1220, July 2006. 3
- [25] Karen Simonyan and Andrew Zisserman. Very deep convolutional networks for large-scale image recognition. In *International Conference on Learning Representations*, 2015. 4
- [26] Jheng-Wei Su, Hung-Kuo Chu, and Jia-Bin Huang. Instance-aware image colorization. In *Proceedings of the IEEE/CVF Conference on Computer Vision and Pattern Recognition (CVPR)*, June 2020. 3
- [27] Carl Vondrick, Abhinav Shrivastava, Alireza Fathi, Sergio Guadarrama, and Kevin Murphy. Tracking emerges by colorizing videos. In *Proceedings of the European Conference on Computer Vision (ECCV)*, September 2018. 2, 3, 5
- [28] Ning Wang, Yibing Song, Chao Ma, Wengang Zhou, Wei Liu, and Houqiang Li. Unsupervised deep tracking. In *Proceedings of the IEEE conference on computer vision and pattern recognition*, pages 1308–1317, 2019. 3
- [29] Xiaolong Wang, Allan Jabri, and Alexei A. Efros. Learning correspondence from the cycle-consistency of time. In *CVPR*, 2019. 3

- [30] Liron Yatziv and Guillermo Sapiro. Fast image and video colorization using chrominance blending. *IEEE transactions on image processing*, 15(5):1120–1129, 2006. 3
- [31] Bo Zhang, Mingming He, Jing Liao, Pedro V. Sander, Lu Yuan, Amine Bermak, and Dong Chen. Deep exemplar-based video colorization. In *Proceedings of the IEEE/CVF Conference on Computer Vision and Pattern Recognition (CVPR)*, June 2019. 1, 3, 4, 6, 7, 8, 11, 12, 13
- [32] Richard Zhang, Phillip Isola, and Alexei A Efros. Colorful image colorization. In *ECCV*, 2016. 3
- [33] Richard Zhang, Jun-Yan Zhu, Phillip Isola, Xinyang Geng, Angela S Lin, Tianhe Yu, and Alexei A Efros. Real-time user-guided image colorization with learned deep priors. *ACM Transactions on Graphics (TOG)*, 9(4), 2017. 3

A. Effect of Reference Frame’s Position

Table 2 shows the results of PSNR on DAVIS-2017 dataset [23], using different reference frame positions from the one reported in the main paper. We only use 30 frames per a video on the single reference setting, since colors that can be specified by a single reference may not include the ground truth colors of distant frames, although more frames can be colored.

As shown in the table, regardless of the reference frame’s position within the video, our model consistently outperforms previous models, demonstrating that it is resilient to the change of reference frame’s position.

B. PSNR on Videvo Dataset

Table 3 shows that our method can better-reflect the colors more from ground truth than the previous methods in Videvo dataset. Videvo dataset includes 60 videos (30 frames/video) that we collected manually from Videvo website¹ such that it includes various scenes. Unlike DAVIS-2017, there is no ground truth segmentation mask, so we only evaluate the entire frame (Full) for each frame. Our observation is that instance detection by MaskRCNN [4] is not successful for Videvo dataset, due to a large number of instances moving or substantial blurs in the background. We suspect that this is why there is no difference in scores between Ours(dense) and Ours(inst.+dense). Also note that, in consistency with Table 2, our model outperforms previous models regardless of the reference frame’s position.

C. Other Evaluation Metric

We report the results with another evaluation metric for reference-based video colorization. The metric we introduce is the percentage of pixels whose error magnitude exceeds a threshold. This is similar to how the KITTI benchmark [22] evaluates the correctness of estimated disparity or flow end-point error (often called % Outlier). In particular, this metric is designed to measure the user controllability. For example, given a case where the creator needs to partially change the color of the area after applying the colorization model, this metric provides a clue as to how much revision will have to be made by the user.

Fig. 11 shows the relationship between the threshold and the percentage of pixels where the error exceeds the threshold. The percentages are averaged across the entire DAVIS-2017 [23] dataset. Ours has consistently fewer errors than other methods. This demonstrates that our method is more similar to ground truth color and realizes better user-controllability and lower costs. For example, in Zhang *et al.* [31]* (linear) vs Ours (inst.+dense), there is a 3.5% difference, when $Threshold = 8$. This implies that at 4K (8.3

million pixels), there is a difference of about 290,000 pixels. In other words, our model leads to reduction of user re-drawing effort of about 540×540 pixels.

Table 4 and Table 5 are the results on DAVIS and Videvo respectively, when we set $Threshold = 16$. Our method performs better than the previous methods, and in particular, we can see that dense tracking is critical for enhancing the performance for the entire image. Fig. 12 and Fig. 13 show visualization of pixels over a threshold of Euclidean distance from ground truth in RGB space, comparing our model with previous models.

¹<https://www.videvo.net>

Single Reference						
Method	1st frame			Nth frame		
	Full	Inner	Outer	Full	Inner	Outer
DeepRemaster [7]	25.34	24.23	25.51	25.31	24.09	25.49
Zhang <i>et al.</i> [31]	28.32	27.48	28.41	28.06	27.21	28.15
Ours (inst.)	28.31	27.52	28.40	28.00	27.21	28.15
Ours (dense)	28.75	27.56	28.87	28.51	27.36	28.64
Ours (inst.+dense)	28.76	27.68	28.88	28.45	27.40	28.63

Table 2: PSNR on DAVIS. Higher is better. We report experiments with two types of reference frames: 1) single reference given at the beginning (1st), and 2) the end (N -th) of a sequence. Full, Inner, and Outer refer to the region with respect to ground truth instance masks used for evaluation.

Method	Single Reference			Multiple References
	1st frame Full	10th frame Full	Nth frame Full	1st & Nth frames Full
DeepRemaster [7]	23.88	24.08	23.85	24.22
Zhang <i>et al.</i> [31]	26.98	27.33	26.77	-
Zhang <i>et al.</i> [31]* (mean)	-	-	-	27.41
Zhang <i>et al.</i> [31]* (linear)	-	-	-	27.63
Ours (w/o tracking)	26.98	27.33	26.77	27.64
Ours (inst.)	26.97	27.32	26.70	27.65
Ours (dense)	27.35	27.76	27.11	28.09
Ours (inst.+dense)	27.35	27.76	27.04	28.10

Table 3: PSNR on Videvo. Higher is better.

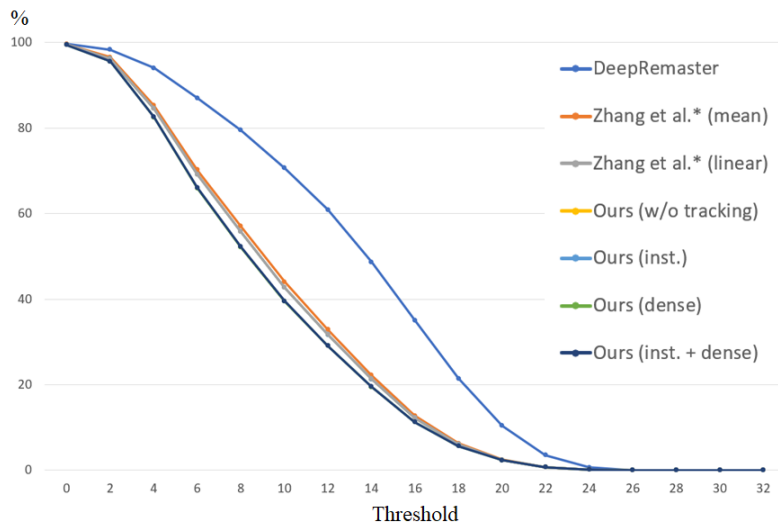


Figure 11: This is the percentage of pixels that is over a threshold of Euclidean distance from ground truth in RGB space.

Method	Single Reference			Multiple References	
	1st	10th	Nth	1st & Nth	10th & N-10th
DeepRemaster [7]	36.0	35.7	35.9	35.3	35.1
Zhang <i>et al.</i> [31]	12.7	12.2	13.0	-	-
Zhang <i>et al.</i> [31]* (mean)	-	-	-	12.8	12.7
Zhang <i>et al.</i> [31]* (linear)	-	-	-	12.5	12.3
Ours (w/o tracking)	12.7	12.2	13.0	12.5	12.2
Ours (inst.)	12.8	12.2	13.0	12.5	12.2
Ours (dense)	11.8	11.0	11.9	11.6	11.2
Ours (inst.+dense)	11.8	11.1	12.0	11.6	11.2

Table 4: % Outlier on DAVIS. Lower is better. This is the percentage of pixels that is over a threshold of Euclidean distance from ground truth in RGB space. We set the *threshold* = 16.

Method	Single Reference			Multiple References
	1st	10th	Nth	1st & Nth
DeepRemaster [7]	38.4	37.8	38.3	37.9
Zhang <i>et al.</i> [31]	14.6	13.6	14.2	-
Zhang <i>et al.</i> [31]* (mean)	-	-	-	13.6
Zhang <i>et al.</i> [31]* (linear)	-	-	-	13.1
Ours (w/o tracking)	14.6	13.6	14.2	12.9
Ours (inst.)	14.6	13.6	14.2	12.9
Ours (dense)	13.8	12.8	13.7	12.1
Ours (inst.+dense)	13.8	12.8	13.7	12.1

Table 5: % Outlier on Videvo. Lower is better. This is the percentage of pixels that is over a threshold of Euclid distance from ground truth in RGB space. We set the *threshold* = 16.

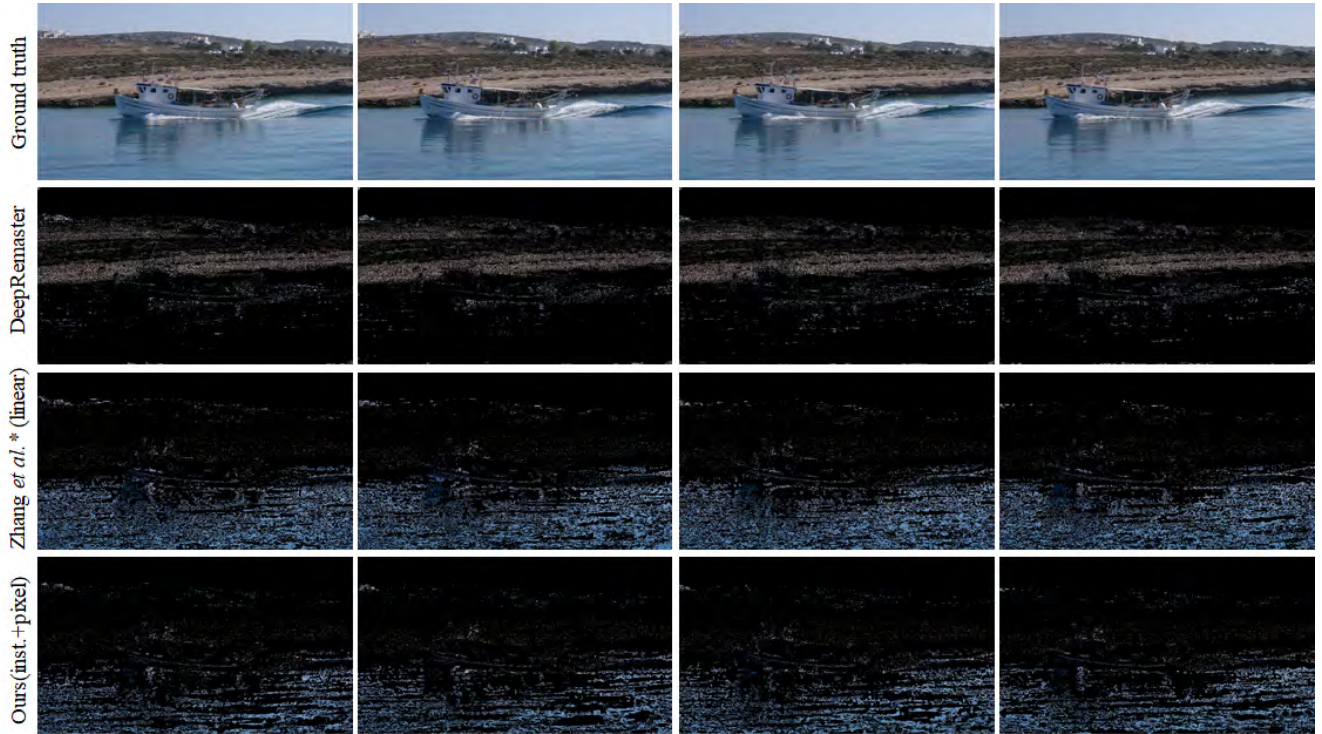


Figure 12: The visualization of the pixels that is over a threshold of Euclidean distance from ground truth in RGB space. We set the $threshold = 16$. Sparser visualization indicates better performance.



Figure 13: The visualization of the pixels that is over a threshold of Euclidean distance from ground truth in RGB space. We set the $threshold = 16$. Sparser visualization indicates better performance.